Supporting Information

Azobenzene-based chloride transporters with light-controllable activities

Ye Rin Choi,[a]‡ Gyu Chan Kim,[a]‡ Hae-Geun Jeon,[a] Jinhong Park,[b] Wan Namkung[b] and Kyu-Sung Jeong[a]*

[a] Department of Chemistry, Yonsei University, Seoul, 120-749, Korea

E-mail: ksjeong@yonsei.ac.kr; Fax: +82-2-364-7050; Tel: +82-2123-2643

[b] College of Pharmacy, Yonsei International Campus, Incheon, 406-840, Korea

‡These authors contributed equally.

Contents

General: All chemicals were purchased from commercial suppliers and used without further purification unless otherwise specified. Dichloromethane (CH_2Cl_2) were purified by drying over calcium hydride (CaH_2), followed by distillation. Hexane, ethyl acetate (EtOAc) and acetone were distilled. Thin layer chromatography (TLC) was performed on Merck (silica gel 60, F-254, 0.25 mm). Silca gel 60 (230-400 mesh, Merck) was used for column chromatography. Melting points were determined with a Barnstead Electrothermal (IA9100) apparatus. NMR spectra were measured by using Bruker DRX 400, Avance II instruments and chemical shifts were reported using residual protonated solvent peaks (for ^{1}H NMR spectra, DMSO-d_6 2.50 ppm; $CDCl_3$ 7.26 ppm and for ^{13}C NMR spectra, DMSO-d_6 39.52 ppm; $CDCl_3$ 77.16 ppm). FT-IR spectra were measured by using a Nicolet Impact-400 FT-IR spectrometer. MALDI-TOF mass spectrometric measurements were performed on a Bruker (LRF20). The elemental analysis data were obtained from *the Yonsei Center for Research Facilities* at Yonsei University and *the Organic Chemistry Research Center* at Sogang University.

1. Syntheses and characterization of new compounds

1.1 Synthesis of compound 13

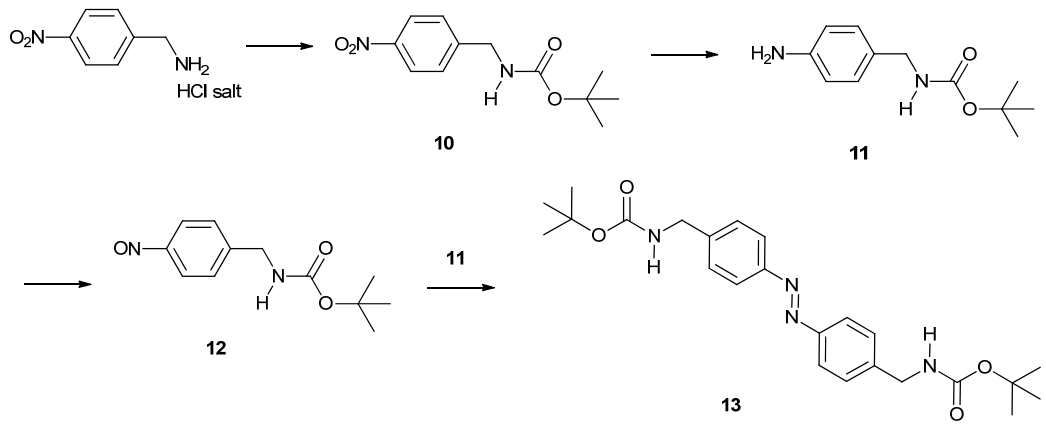

***tert*-Butyl 4-nitrobenzylcarbamate (10)**: Di-*tert*-butyl dicarbonate (12.2 mL, 1 equiv) was added to a solution of 4-nitrobenylamine hydrochloride (10.0 g, 53.0 mmol) and Et_3N (22.2 mL, 3.00 equiv) in EtOH (250 mL), and the solution was stirred vigorously for 4 h at

ambient conditions[S1]. The solution was concentrated and the residue was dissolved in ethyl acetate (EtOAc). The solution was washed with water (100 mL x 3), dried over anhydrous Na_2SO_4, and filtered. After the solvent was removed, the crude product was purified by flash column chromatography (silica gel, EtOAc:hexane, 1:2 v/v) to give compound **10** as a white solid. (11.2 g, 84%); mp: 110–111 °C; TLC (EtOAc:hexane, 1:2 v/v): R_f= 0.39; ^{1}H NMR (400 MHz, $CDCl_3$, 298 K, ppm) δ 8.19 (d, J = 8.5 Hz, 2H), 7.44 (d, J = 8.2 Hz, 2H), 4.99 (br, 1H, NH), 4.41(d, J = 4.9 Hz, 2H), 1.47 (s, 9H); ^{13}C NMR (100 MHz, $CDCl_3$, 298 K, ppm) δ 156.1, 147.4, 146.9, 128.0, 124.0, 80.3, 44.2, 28.5; IR (KBr pellet): 3328 (NH), 1689 (C=O) cm^{-1}.

***tert*-Butyl 4-aminobenzylcarbamate (11)**: Compound **10** (11.0 g, 43.6 mmol) was transferred into a flask containing Pd/C 10% (0.23 g, 0.05 equiv) dispersed in EtOAc (250 mL). The mixture was stirred under H_2 (g) for 1 h at room temperature[S2]. The catalyst was filtered out through Celite and the solvent was evaporated. The crude mixture was purified by flash column chromatography (silica gel, EtOAc:hexane, 1:2 v/v) to afford **11** as a white solid (9.50 g, 98%); mp: 79–80 °C; TLC (EtOAc:hexane, 1:2 v/v): R_f= 0.18; ^{1}H NMR (400 MHz, $CDCl_3$, 298 K, ppm) δ 7.07 (d, J = 8.1 Hz, 2H), 6.64 (d, J = 8.3 Hz, 2H), 4.70 (br, 1H, NH), 4.18 (d, J = 5.1 Hz, 2H), 3.64 (s, 2H, NH), 1.45 (s, 9H); ^{13}C NMR (100 MHz, $CDCl_3$, 298 K, ppm) δ 155.9, 145.8, 128.8, 128.7, 115.2, 79.2, 44.3, 20.5; IR (KBr pellet): 3428 (NH_2), 3346 (NH), 1689 (C=O) cm^{-1}.

***tert*-Butyl 4-nitrosobenzylcarbamate (12)**: A solution of **11** (6.00 g, 27.0 mmol) in CH_2Cl_2 (100 mL) was added to a solution of oxone (33.2 g, 2.00 equiv) in H_2O (300 mL)[S3,4]. The two layered solution was stirred fiercely under nitrogen for 3 h at room temperature, while the color of the solution was gradually turned into green as the desired nitroso compound formed. After separation of the layers, aqueous layer was extracted with CH_2Cl_2. The

[S1] (a) T. W. Green, P. G. M. Wuts, In *Protective Groups in Organic Synthesis*, Wiley-Interscience: New York, 1999; pp 518–525, pp 736–739; (b) S. V. Chankeshwara and A. K. Chakraborti, *Org. Lett*., 2006, **8**, 3259–3262.
[S2] G. S. Vanier, *Synlett*., 2007, **1**, 131–135.
[S3] B.-C. Yu and Y. Shirai, J. M. Tour, *Tetrahedron,* 2006, **62**, 10303–10310.
[S4] B. Priewisch and K. Ruck-Braun, *J. Org. Chem*., 2005, **70**, 2350–2352.

organic layers were dried over anhydrous Na_2SO_4, and concentrated. The crude mixture was purified by flash column chromatography (silica gel, EtOAc:hexane, 1:2 v/v) to afford **12** as a bluish green solid (3.57 g, 56%); mp: 82–83 °C; TLC (EtOAc:hexane, 1:2 v/v): R_f= 0.46; ^{1}H NMR (400 MHz, $CDCl_3$, 298 K, ppm) δ 7.87 (d, J = 8.1 Hz, 2H), 7.51 (d, J = 8.5 Hz, 2H), 4.99 (br, 1H, NH), 4.40 (d, J = 5.4 Hz, 2H), 1.47 (s, 9H); ^{13}C NMR (100 MHz, $CDCl_3$, 298 K, ppm) δ 156.0, 147.5, 127.7, 123.8, 121.4, 80.0, 44.2, 28.4; IR (KBr pellet): 3350 (NH), 1680 (C=O) cm^{-1}.

***tert*-Butyl (4,4'-(diazene-1,2-diyl)bis(4,1-phenylene))bis(methylene)dicarbamate (13):** A solution of **11** (3.00 g, 13.5 mmol) and **12** (3.19 g, 1.00 equiv) in acetic acid (100 mL) was stirred for 6 h[S3,4], and the solution was diluted with CH_2Cl_2 (200 mL). The solution was basified carefully with a saturated $NaHCO_3$ solution. The organic layer was washed with a saturated $NaHCO_3$ solution and dried over anhydrous Na_2SO_4. The solvent was removed and the crude product was purified by flash column chromatography (silicagel, EtOAc:hexane, 1:2 v/v) to afford **13** as an orange solid (4.40 g, 74%); mp: 197–198 °C; TLC (EtOAc:hexane, 1:2 v/v): R_f= 0.35 (*trans*) and 0.18 (*cis* isomers); ^{1}H NMR (400 MHz, $CDCl_3$, 298 K, ppm) δ 7.87 (d, J = 8.0 Hz, 2H), 7.42 (d, J = 8.3 Hz, 2H), 4.91 (br, 1H, NH), 4.40 (d, J = 4.9 Hz, 2H), 1.48 (s, 9H); ^{13}C NMR (100 MHz, DMSO-d_6, 298 K, ppm) δ 156.3, 151.3, 144.3, 128.3, 123.0, 78.4, 43.6, 28.7; IR (KBr pellet): 3345 (NH), 1686 (C=O) cm^{-1}. MALDI-TOF (*m/z*): $[M+H]^+$ calcd. for $C_{24}H_{32}N_4O_4$, 441.2; found, 441.2; analysis (calcd., found for $C_{24}H_{32}N_4O_4$): C (65.43, 65.45), H (7.32, 7.28), N (12.72, 12.79).

1.2 Synthesis of compounds **1**-7

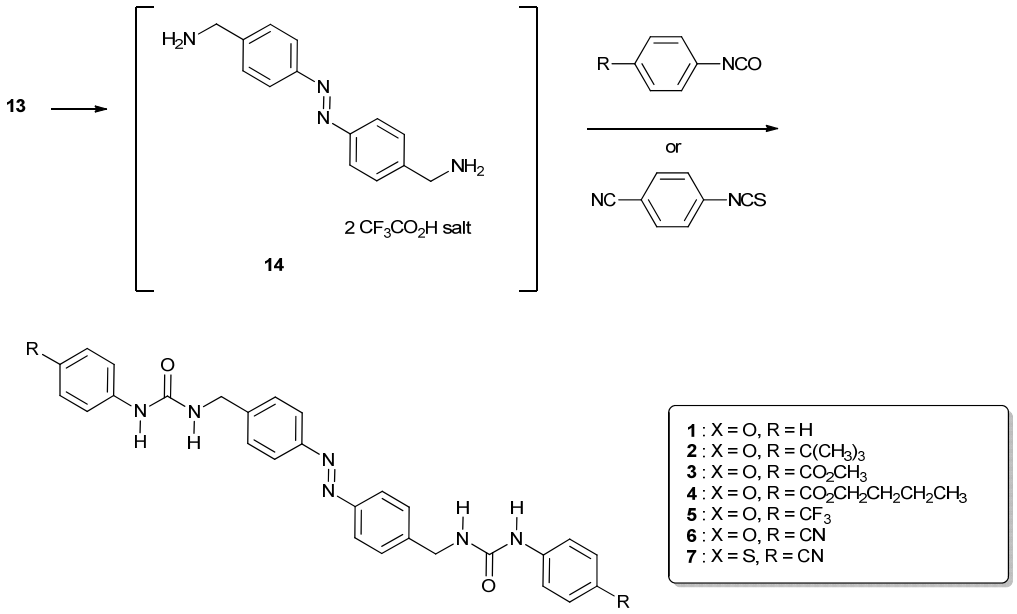

Trifluoroacetic acid (CF_3CO_2H, 3.5 mL, 5 equiv) was added to a solution of **13** (4.0 g, 9.1 mmol) in CH_2Cl_2 (90 mL) and the solution was stirred for 8 h at room temperature [S5]. The suspension was filtered and the filter cake was washed repeatedly with CH_2Cl_2 and toluene to afford **14** as an orange solid (4.1 g, 97%); ^{1}H NMR (400 MHz, DMSO-d_6, 298 K, ppm) δ 8.32 (s, 6H, NH), 7.95 (d, J = 8.4 Hz, 4H), 7.68 (d, J = 8.6 Hz, 4H), 4.17 (br, 4H).

This crude product was directly used for next reaction without further purification.

Compound 1: Phenyl isocyanate (0.16 mL, 2 equiv) was added to a solution of **14** (0.30 g, 0.64 mmol), Et_3N (0.45 mL, 5 equiv) in CH_2Cl_2 (5 mL), and the solution was stirred overnight at room temperature while the product was solidified out. The suspension was filtered and the filter cake was washed repeatedly with CH_2Cl_2 and water. The crude product was purified by re-crystallizing from a mixture solution of *N,N*-dimethyl formamide (DMF), acetone and hexane, affording **1** as a orange solid (0.29 g, 93%); mp: 306–307 °C (dec); ^{1}H NMR (400 MHz, DMSO-d_6, 298 K, ppm) δ 8.65 (s, 2H, NH), 7.87 (d, J = 8.5 Hz, 4H), 7.50 (d, J = 8.3 Hz, 4H), 7.41 (d, J = 7.8 Hz, 4H), 7.22 (t, J = 7.8 Hz, 4H), 6.89 (t, J = 7.3 Hz, 2H), 6.73 (t, J = 5.9 Hz, 2H, NH), 4.40 (d, J = 5.8 Hz, 4H); ^{13}C

[S5] S. Natarajan, A. Yurek-George and A. Ganesan, *Molecular Diversity*, 2005, **9**, 291–293.

NMR (100 MHz, DMSO-d_6, 298 K, ppm) δ 155.7, 151.3, 144.6, 140.8, 129.1, 128.4, 123.0, 121.6, 118.3, 42.9; IR (KBr pellet): 3307 (NH), 1631 (C=O) cm^{-1}; MALDI-TOF (*m/z*) [M^+] calcd. for $C_{28}H_{26}N_6O_2$, 478.2; found, 478.7; analysis (calcd., found for $C_{28}H_{26}N_6O_2$): C (70.28, 70.31), H (5.48, 5.58), N (17.56, 17.76).

Compound 2: 4-*tert*-Butyl aniline (0.26 mL, 2.5 equiv) and triphosgene (0.20 g, 0.4 equiv of aniline) were sequentially added in CH_2Cl_2 (10 mL) and saturated $NaHCO_3$ aqueous solution (10 mL). Two-layered solution was stirred for 30 min at room temperature and separated. The organic layer was dried over anhydrous Na_2SO_4 and transferred to a solution of **14** (0.30 g, 0.64 mmol) and Et_3N (0.45 mL, 5 equiv) in CH_2Cl_2 (5 mL). The solution was stirred overnight at room temperature while a solid product was precipitated out. The crude product was purified by re-crystallizing from a mixture solution of *N,N*-dimethyl formamide (DMF), acetone and hexane, affording **2** as a orange solid (0.33 g, 87%); mp: 294–295 °C (dec); ^{1}H NMR (400 MHz, DMSO-d_6, 298 K, ppm) δ 8.56 (s, 2H, NH), 7.86 (d, J = 8.1 Hz, 4H), 7.49 (d, J = 8.1 Hz, 4H), 7.32 (d, J = 8.6 Hz, 4H), 7.24 (d, J = 8.4 Hz, 4H), 6.67 (t, J = 5.8 Hz, 2H, NH), 4.39 (d, J = 5.7 Hz, 4H), 1.24 (s, 18H); ^{13}C NMR (100 MHz, DMSO-d_6, 298 K, ppm) δ 155.9, 151.3, 144.8, 143.9, 138.2, 128.5, 125.7, 123.0, 118.1, 43.0, 34.3, 31.9; IR (KBr pellet): 3347 (NH), 1699 (C=O) cm^{-1}; MALDI-TOF (*m/z*): $[M+H]^+$ calcd. for $C_{36}H_{42}N_6O_2$, 591.3; found, 591.6; analysis (calcd., found for $C_{36}H_{42}N_6O_2$): C (73.19, 73.07), H (7.17, 7.23), N (14.23, 13.99).

Compounds **3-7** were prepared from the corresponding *para*-substituted anilines instead of *tert*-butyl aniline, following the procedure described for the preparation of compound **2**.

Compound 3: An orange solid (88% yield); mp: 298–299 °C; ^{1}H NMR (400 MHz, DMSO-d_6, 298 K, ppm) δ 9.14 (s, 2H, NH), 7.87 (d, J = 8.6 Hz, 4H), 7.84 (d, J = 9.2 Hz, 4H), 7.55 (d, J = 8.8 Hz, 4H), 7.51 (d, J = 8.3 Hz, 4H), 6.93 (t, J = 5.8 Hz, 2H, NH), 4.41 (d, J = 5.8 Hz, 4H), 3.80 (s, 6H) ; ^{13}C NMR (100 MHz, DMSO-d_6, 298 K, ppm) δ 166.5, 155.4, 151.4, 145.6, 144.4, 130.8, 128.5, 123.1, 122.3, 117.3, 52.1, 43.0; IR (KBr pellet): 3312 (NH), 1720 (C=O) cm^{-1}; MALDI-TOF (*m/z*): [M^+] calcd. for $C_{32}H_{30}N_6O_6$, 594.2; found, 594.8; analysis (calcd., found for $C_{32}H_{30}N_6O_6$): C (64.64, 64.59), H (5.09, 5.16), N (14.13,

14.25).

Compound 4: An orange solid (87% yield); mp: 244–245 °C (dec); ^{1}H NMR (400 MHz, DMSO-d_6, 298 K, ppm) δ 9.14 (s, 2H, NH), 7.87 (d, J = 8.3 Hz, 4H), 7.83 (d, J = 8.7 Hz, 4H), 7.55 (d, J = 8.9 Hz, 4H), 7.51 (d, J = 8.3 Hz, 4H), 6.91 (t, J = 5.7 Hz, 2H, NH), 4.42 (d, J = 5.6 Hz, 4H), 4.22 (t, J = 6.3 Hz, 4H), 1.67 (quin, J = 7.2 Hz, 4H), 1.40 (sex, J = 7.5 Hz, 4H), 0.93 (t, J = 7.6 Hz, 6H); ^{13}C NMR (100 MHz, DMSO-d_6, 298 K, ppm) δ 166.0, 155.3, 151.4, 145.5, 144.4, 130.8, 128.6, 123.1, 122.6, 117.4, 64.7, 43.2, 31.0, 19.3, 14.3; IR (KBr pellet): 3347 (NH) cm^{-1}, 1703 (C=O) cm^{-1}; MALDI-TOF (*m/z*): [M+H]$^{+}$ calcd. for $C_{38}H_{42}N_6O_6$, 679.3; found, 679.6; analysis (calcd., found for $C_{38}H_{42}N_6O_6$): C (67.24, 67.04), H (6.24, 6.31), N (12.38, 12.42).

Compound 5: An orange solid (64% yield); mp: 297–298 °C (dec); ^{1}H NMR (400 MHz, DMSO-d_6, 298 K, ppm) δ 9.14 (s, 2H, NH), 7.87 (d, J = 8.3 Hz, 4H), 7.62 (d, J = 8.9 Hz, 4H), 7.57 (d, J = 8.9 Hz, 4H), 7.51 (d, J = 8.3 Hz, 4H), 6.92 (t, J = 6.1 Hz, 2H, NH), 4.42 (d, J = 5.9 Hz, 4H); ^{13}C NMR (100 MHz, DMSO-d_6, 298 K, ppm) δ 155.1, 151.0, 144.2, 144.0, 128.1, 126.1, 122.8, 121.5, 121.2, 117.6, 42.6; IR (KBr pellet): 3315 (NH), 1636 (C=O) cm^{-1}; MALDI-TOF (*m/z*): [M^{+}] calcd. for $C_{30}H_{24}F_6N_6O_2$, 614.2; found, 614.9; analysis (calcd., found for $C_{30}H_{24}F_6N_6O_2$): C (58.63, 58.88), H (3.94, 4.08), N (13.68, 13.81).

Compound 6: An orange solid (74% yield); mp: 289–290 °C (dec); ^{1}H NMR (400 MHz, DMSO-d_6, 298 K, ppm) δ 9.25 (s, 2H, NH), 7.87 (d, J = 8.2 Hz, 4H), 7.68 (d, J = 8.5 Hz, 4H), 7.60 (d, J = 8.8 Hz, 4H), 7.51 (d, J = 8.3 Hz, 4H), 6.99 (t, J = 6.0 Hz, 2H, NH), 4.42 (d, J = 5.5 Hz, 4H); ^{13}C NMR (100 MHz, DMSO-d_6, 298 K, ppm) δ 155.2, 151.4, 145.3, 144.2, 133.6, 128.4, 123.0, 119.9, 118.0, 103.0, 42.9; IR (KBr pellet): 3325 (NH), 2223 (C≡N), 1639 (C=O) cm^{-1}; MALDI-TOF (*m/z*): [M^{+}] calcd. for $C_{30}H_{24}N_8O_2$, 528.2; found, 528.7; analysis (calcd., found for $C_{30}H_{24}N_8O_2$): C (68.17, 68.39), H (4.58, 4.64), N (21.20, 20.95).

Compound 7: An orange solid (89% yield); mp: 230–231 °C; ^{1}H NMR (400 MHz, DMSO-d_6, 298 K, ppm) δ 10.18 (s, 2H, NH), 8.71 (br, 2H, NH), 7.88 (d, J = 8.1 Hz, 4H), 7.78 (s, 8H), 7.55 (d, J = 8.2 Hz, 4H), 4.87 (br, 4H); ^{13}C NMR (100M Hz, DMSO-d_6, 298 K, ppm) δ 181.1, 151.5, 144.5, 142.7, 133.3, 128.8, 123.1, 122.1, 119.6, 105.4, 47.2; IR (KBr pellet): 3353 (NH), 2229 (C≡N), 1239 (C=S) cm^{-1}; MALDI-TOF (*m/z*): [M^{+}] calcd.

for $C_{30}H_{24}N_8S_2$, 560.1; found, 560.7; analysis (calcd., found for $C_{30}H_{24}N_8S_2$): C (64.26, 64.24), H (4.31, 4.28), N (19.98, 19.95), S (11.44, 11.64).

1.3 Synthesis of compound 18

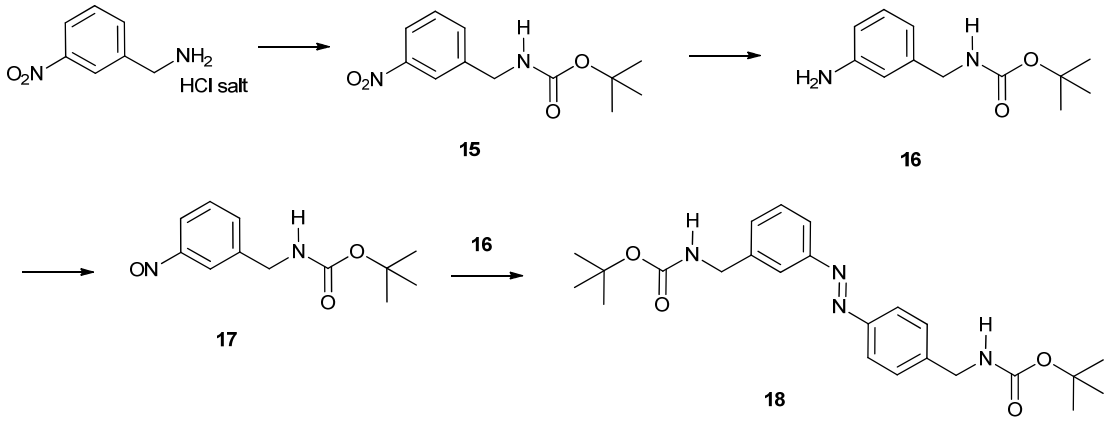

Compound **18** was prepared following the procedures described earlier for the preparation of analogous compound **13**.

***tert*-Butyl 3-nitrobenzylcarbamate (15)**: **A** white solid (90% yield); mp: 86–87 °C; TLC (EtOAc:hexane, 1:2 v/v): R_f= 0.44; ^{1}H NMR (400 MHz, DMSO-d_6, 298 K, ppm) δ 8.10 (d, J = 7.1 Hz, 1H), 8.09 (s, 1H), 7.69 (d , J = 7.6 Hz, 1H), 7.62 (t , J = 8.5 Hz, 1H), 7.57 (t , J = 8.0 Hz, 1H, NH), 4.25 (d, J = 6.3 Hz, 2H), 1.40 (s, 9H); ^{13}C NMR (100 MHz, DMSO-d_6, 298 K, ppm) δ 155.9, 147.8, 142.7, 133.8, 129.9, 121.8, 121.4, 78.2, 42.8, 28.2; IR (KBr pellet): 3353 (NH), 1686 (C=O) cm^{-1}.

***tert*-Butyl 3-aminobenzylcarbamate (16)**: **A**n oily liquid (97% yield); TLC (EtOAc:hexane, 1:2 v/v): R_f= 0.22; ^{1}H NMR (400 MHz, DMSO-d_6, 298 K, ppm) δ 7.26 (t, J = 6.0 Hz, 1H, NH), 6.92 (t, J = 7.6 Hz, 1H), 6.41 (s, 1H), 6.39 (d, J = 7.8 Hz, 1H), 6.35 (d, J = 7.6 Hz, 1H), 5.02 (s, 2H, NH), 3.96 (d, J = 6.1 Hz, 2H), 1.39 (s, 9H); ^{13}C NMR (100 MHz, DMSO-d_6, 298 K, ppm) δ 155.9, 148.6, 140.9, 128.8, 114.7, 112.6, 112.5, 77.8, 43.7, 28.4; IR (KBr pellet): 3449 (NH), 3368 (NH_2), 1676 (C=O) cm^{-1}.

***tert*-butyl 3-nitrosobenzylcarbamate (17)**: An oily liquid (59% yield); TLC (EtOAc:hexane, 1:2 v/v): R_f= 0.32; ^{1}H NMR (400 MHz, DMSO-d_6, 298 K, ppm) δ 7.95 (d,

J = 5.9 Hz, 1H), 7.75 (s, 1H), 7.73 (d, J = 5.7 Hz, 1H), 7.65 (t, J = 8.7 Hz, 1H), 7.58 (t, J = 6.4 Hz, 1H, NH), 4.28 (d, J = 5.7 Hz, 2H), 1.41 (s, 9H); ^{13}C NMR (100 MHz, DMSO-d_6, 298 K, ppm) δ 166.3, 156.0, 142.4, 134.9, 129.8, 120.6, 117.8, 78.1, 42.9, 28.2; IR (KBr pellet): 3343 (NH), 1694 (C=O) cm^{-1}.

***tert*-Butyl (3,3'-(diazene-1,2-diyl)bis(3,1-phenylene))bis(methylene)dicarbamate (18):** An orange solid (72% yield); mp: 129–130 °C; TLC (EtOAc:CH_2Cl_2, 1:5 v/v): R_f = 0.35 (*trans*) and 0.25 (*cis* isomers); ^{1}H NMR (400 MHz, DMSO-d_6, 298 K, ppm) δ 7.77 (d, J = 7.4 Hz, 1H), 7.75 (s, 2H), 7.56 (t, J = 7.6 Hz, 2H, NH), 7.54 (d, J = 7.6 Hz, 2H), 7.43 (d, J = 7.6 Hz, 2H), 4.24 (d, J = 6.5 Hz, 4H), 1.41 (s, 18H); ^{13}C NMR (100 MHz, DMSO-d_6, 298 K, ppm) δ 156.0, 152.0, 141.9, 130.2, 129.4, 121.9, 120.1, 78.0, 43.2, 28.3; IR (KBr pellet): 3363 (NH), 1684 (C=O) cm^{-1}. MALDI-TOF (*m/z*): $[M+H]^+$ calcd. for $C_{24}H_{32}N_4O_4$, 441.2; found, 441.2; analysis (calcd., found for $C_{24}H_{32}N_4O_4$): C (65.43, 65.43), H (7.32, 7.44), N (12.72, 12.75).

1.4 Synthesis of compounds 8 and 9

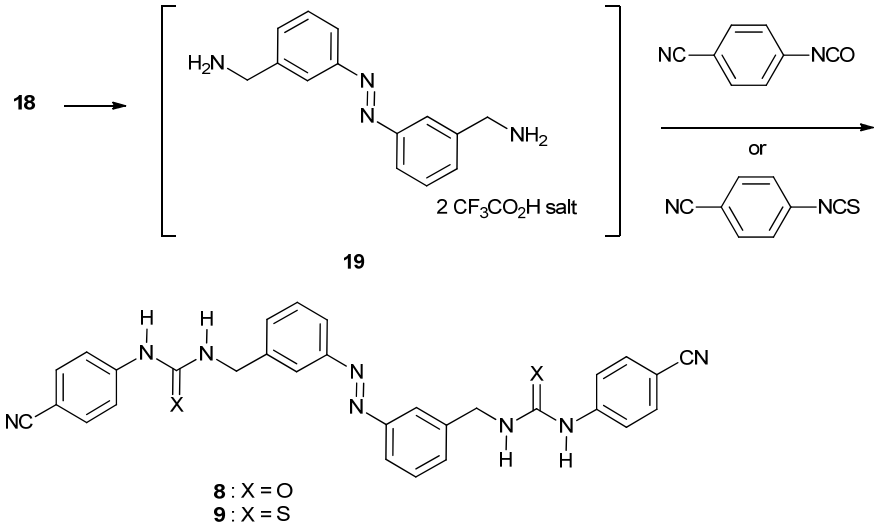

Compounds **8** and **9** were prepared following the procedures described earlier for the preparation of compounds **6** and **7**.

Compound 8: An orange solid (0.28 g, 82%); mp 258–259 °C; ^{1}H NMR (400 MHz,

DMSO-d_6, 298 K, ppm) δ 9.24 (s, 2H, NH), 7.83 (s, 2H), 7.78 (d, J = 7.8 Hz, 2H), 7.67 (d, J = 8.7 Hz, 4H), 7.59 (d, J = 8.7 Hz, 4H), 7.56 (t, J = 7.6 Hz, 2H), 7.51 (d, J = 7.2 Hz, 2H), 7.02 (t, J = 5.9 Hz, 2H, NH), 4.43 (d, J = 5.9 Hz, 4H); ^{13}C NMR (100 MHz, DMSO-d_6, 298 K, ppm) δ; 155.4, 152.4, 145.4, 142.1, 133.8, 131.0, 130.1, 121.8, 121.4, 119.8, 118.2, 103.2, 43.2; IR (KBr pellet): 3317 (NH), 2225 (C≡N), 1644 (C=O) cm^{-1}; MALDI-TOF (*m/z*): $[M+H]^+$ calcd. for $C_{30}H_{24}N_8O_2$, 529.2; found, 529.4; analysis (calcd., found for $C_{30}H_{24}N_8O_2$): C (68.17, 68.13), H (4.58, 4.61), N (21.20, 21.16).

Compound 9: An orange solid (78% yield); mp: 218–219 °C; ^{1}H NMR (400 MHz, DMSO-d_6, 298 K, ppm) δ 10.15 (s, 2H, NH), 8.73 (br, 2H, NH), 7.87 (s, 2H), 7.80 (d, J = 7.3 Hz, 2H), 7.76 (br, 8H), 7.59 (t, J = 7.1 Hz, 2H), 7.57 (d, J = 7.6 Hz, 2H), 4.88 (br, 4H); ^{13}C NMR (100 MHz, DMSO-d_6, 298 K, ppm) δ; 181.1, 152.4, 144.6, 140.7, 133.3, 131.2, 130.0, 122.1, 121.9, 121.8, 119.6, 105.4, 47.2; IR (KBr pellet): 3348 (NH), 2226 (C≡N), 1239 (C=S) cm^{-1}; MALDI-TOF (*m/z*): $[M+H]^+$ calcd. for $C_{30}H_{24}N_8S_2$, 561.2; found, 561.3; analysis (calcd., found for $C_{30}H_{24}N_8S_2$): C (64.26, 64.25), H (4.31, 4.43), N (19.98, 19.86), S (11.44, 11.38).

2. Partial ^{1}H NMR and UV/Vis spectra of *cis* and *trans* isomers

UV/Vis spectra: Each stock solution (20 μM in DMSO) of compounds **1-9** was prepared in a vial covered with aluminum foil, and 2 mL of the solution was transferred to a UV cell and an initial spectrum was recorded (Agilent 8453 UV-Visible spectrophotometer) for the *trans* isomer. Next, the solution was irradiated with a UV lamp (BLACK-RAY 100W mercury spot lamp, 365 nm), which resulted in *trans*-to-*cis* isomerisation. The isomerisation was completed within 1 min and the UV/vis spectra remained unchanged afterwards.

^{1}H NMR spectra: Each stock solution (4 mM in DMSO-d_6) of compounds **1-9** was prepared in a vial covered with aluminum foil. An aliquot (500 μL) of the solution was transferred to a NMR tube and ^{1}H NMR spectrum was recorded for the *trans* isomer. An aliquot (500-1000 μL) of the stock solution was transferred to a quartz cell and irradiated for 3-5 min with a UV lamp (BLACK-RAY 100W mercury spot lamp, 365 nm), which resulted in *trans*-to-*cis* isomerisation. ^{1}H NMR spectrum was recorded and the population of the *cis* isomer at the photo-stationary state (PSS's) was determined by the ^{1}H NMR integration of properly resolved benzylic CH signals (4.5-5 ppm).

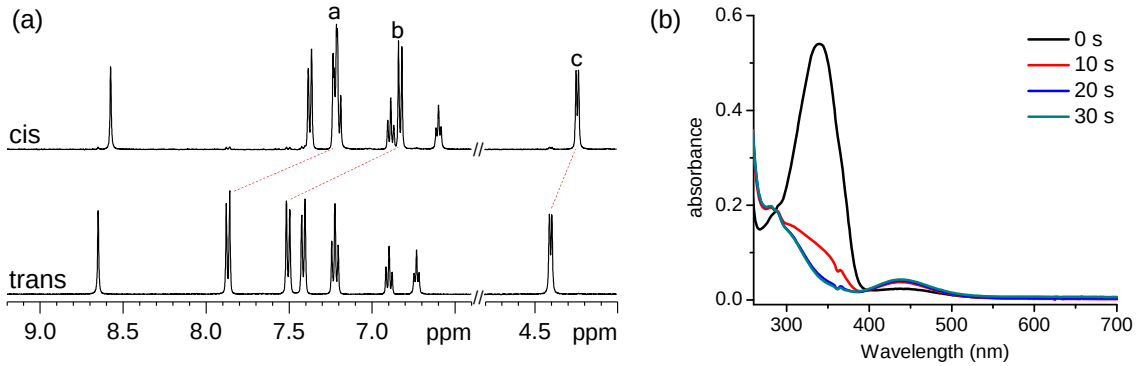

Figure S1. (a) partial ^{1}H NMR spectra (400 MHz, 4.0 × 10^{-3} M in DMSO-d_6, 25 °C) of *trans*-**1** (down) and *cis*-**1** (up); *trans* : *cis* = 4 : 96 at PSS. (b) UV/Vis absorption spectral changes of **1** (2.0 × 10^{-5} M in DMSO, 25 °C) upon irradiation at 365 nm.

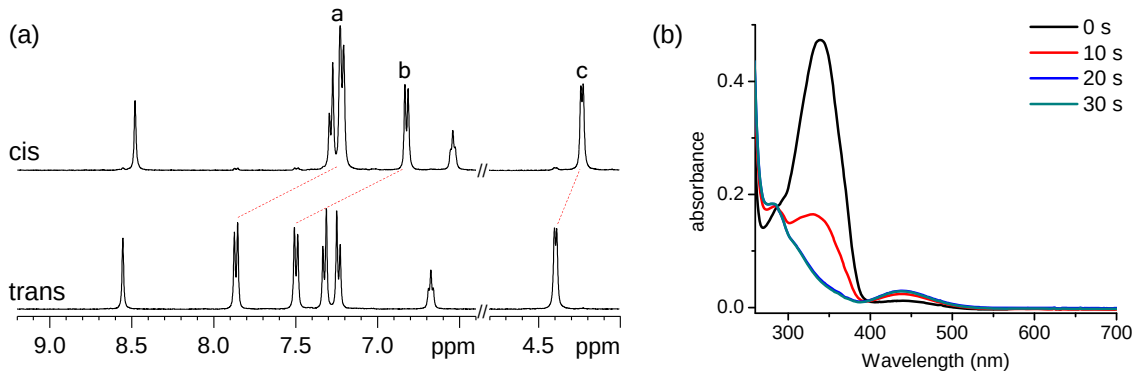

Figure S2. (a) partial ^{1}H NMR spectra (400 MHz, 4.0 × 10^{-3} M in DMSO-d_6, 25 °C) of *trans*-**2** (down) and *cis*-**2** (up); *trans* : *cis* = 4 : 96 at PSS. (b) UV/Vis absorption spectral changes of **2** (2.0 × 10^{-5} M in DMSO, 25 °C) upon irradiation at 365 nm.

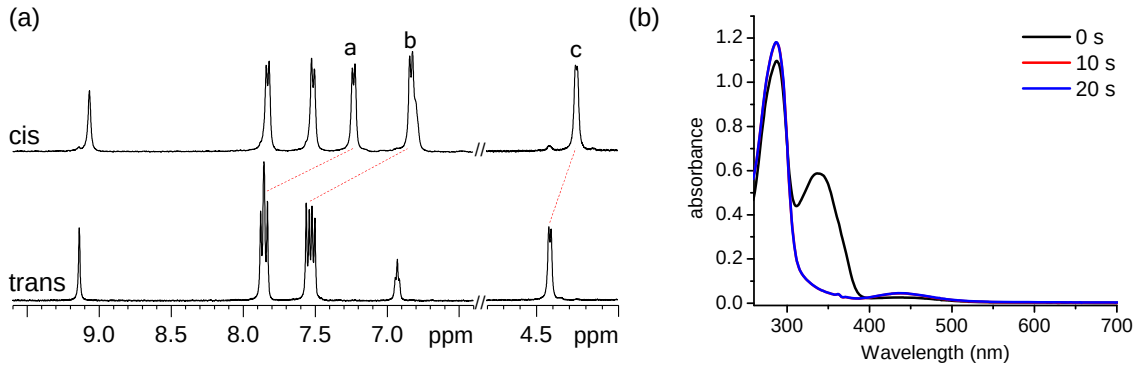

Figure S3. (a) partial ^{1}H NMR spectra (400 MHz, 4.0 × 10^{-3} M in DMSO-d_6, 25 °C) of *trans*-**3** (down) and *cis*-**3** (up); *trans* : *cis* = 4 : 96 at PSS. (b) UV/Vis absorption spectral changes of **3** (2.0 × 10^{-5} M in DMSO, 25 °C) upon irradiation at 365 nm.

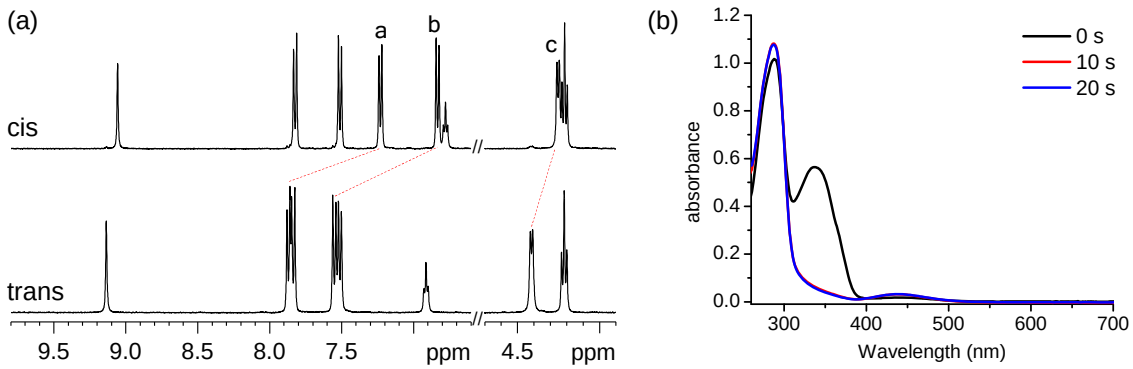

Figure S4. (a) partial ^{1}H NMR spectra (400 MHz, 4.0 × 10^{-3} M in DMSO-d_6, 25 °C) of *trans*-**4** (down) and *cis*-**4** (up); *trans*/*cis* = 4 : ~96 at PSS. (b) UV/Vis absorption spectral changes of **4** (2.0 × 10^{-5} M in DMSO, 25 °C) upon irradiation at 365 nm.

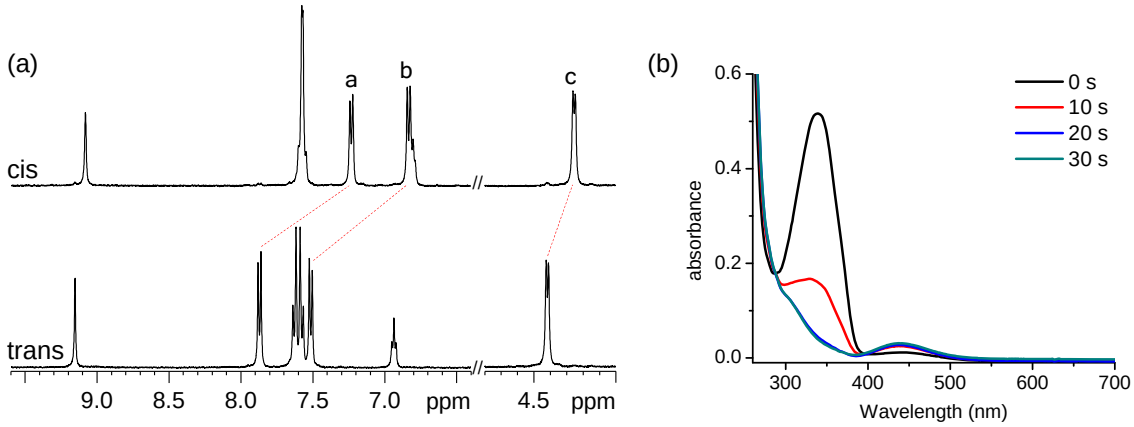

Figure S5. (a) partial ^{1}H NMR spectra (400 MHz, 4.0 × 10^{-3} M in DMSO-d_6, 25 °C) of *trans*-**5** (down) and *cis*-**5** (up); *trans* : *cis* = 5 : 95 at PSS. (b) UV/Vis absorption spectral changes of **5** (2.0 × 10^{-5} M in DMSO, 25 °C) upon irradiation at 365 nm.

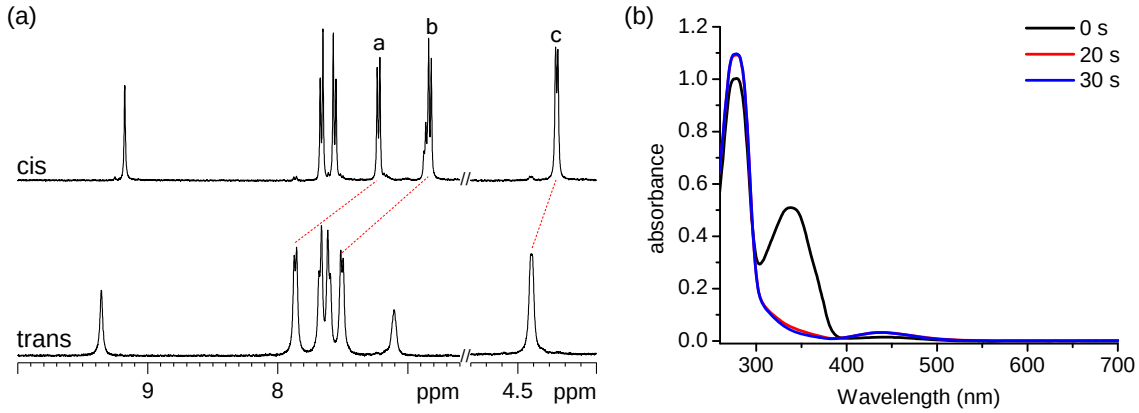

Figure S6. (a) partial ^{1}H NMR spectra (400 MHz, 4.0 × 10^{-3} M in DMSO-d_6, 25 °C) of *trans*-**6** (down) and *cis*-**6** (up); *trans* : *cis* = 4 : 96 at PSS. (b) UV/Vis absorption spectral changes of **6** (2.0 × 10^{-5} M in DMSO, 25 °C) upon irradiation at 365 nm.

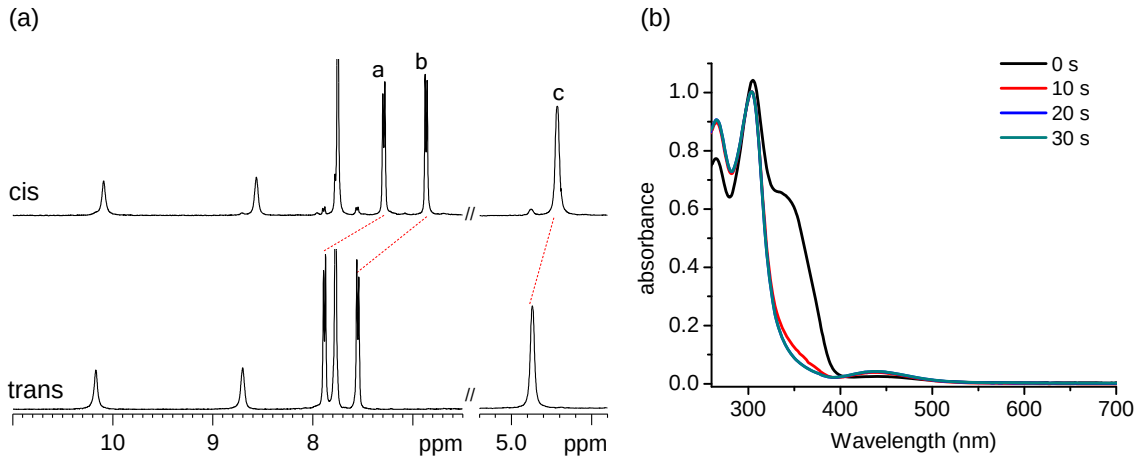

Figure S7. (a) partial ^{1}H NMR spectra (400 MHz, 4.0 × 10^{-3} M in DMSO-d_6, 25 °C) of *trans*-**7** (down) and *cis*-**7** (up); *trans* : *cis* = 8 : 92 at PSS. (b) UV/Vis absorption spectral changes of **7** (2.0 × 10^{-5} M in DMSO, 25 °C) upon irradiation at 365 nm.

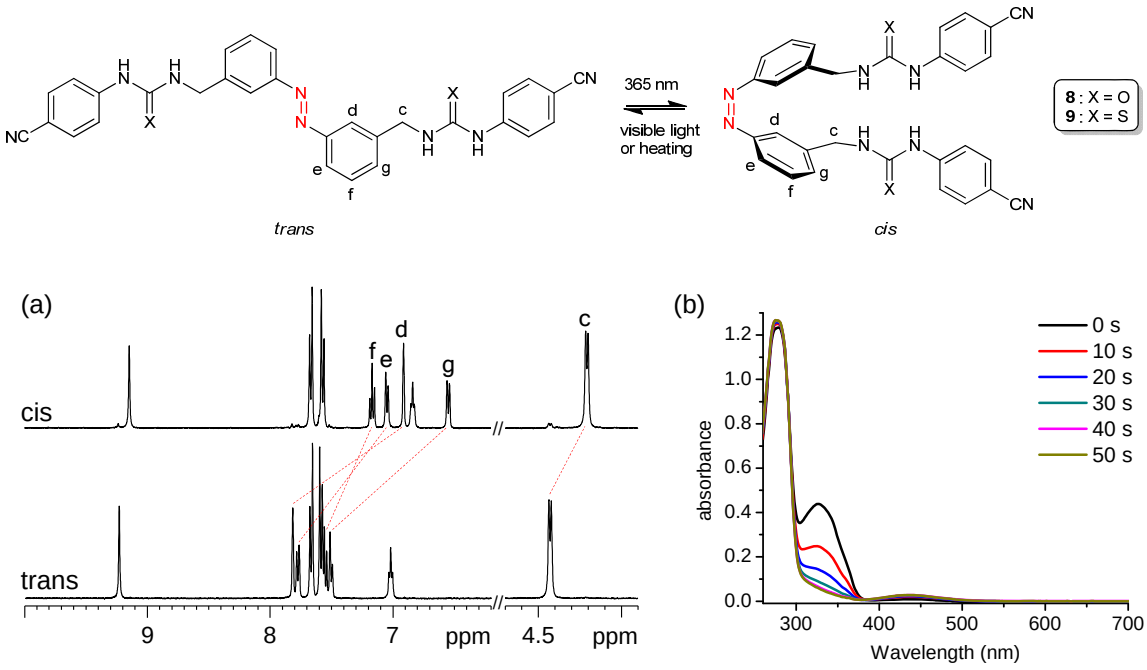

Figure S8. (a) partial ^{1}H NMR spectra (400 MHz, 4.0 × 10^{-3} M in DMSO-d_6, 25 °C) of *trans*-**8** (down) and *cis*-**8** (up); *trans* : *cis* = 4 : 96 at PSS. (b) UV/Vis absorption spectral changes of **8** (2.0 × 10^{-5} M in DMSO, 25 °C) upon irradiation at 365 nm.

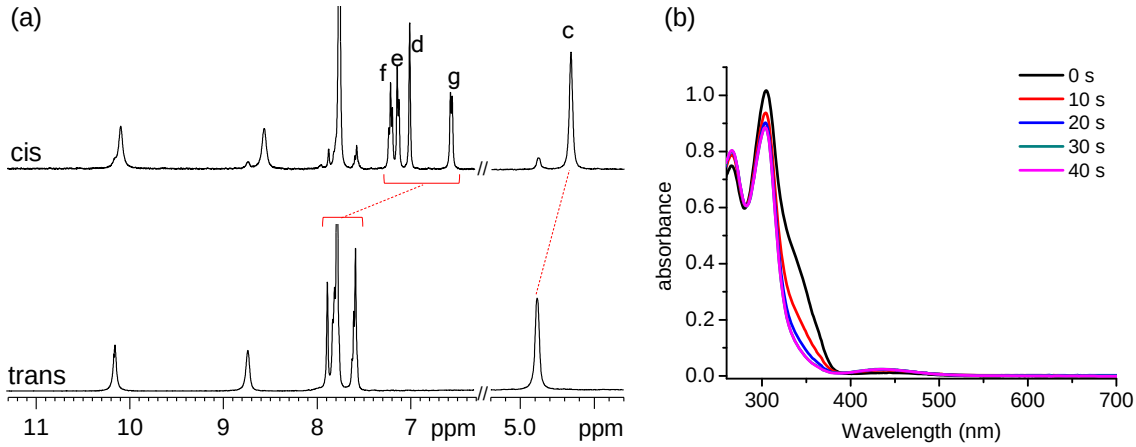

Figure S9. (a) partial ^{1}H NMR spectra (400 MHz, 4.0 × 10^{-3} M in DMSO-d_6, 25 °C) of *trans*-**9** (down) and *cis*-**9** (up); *trans* : *cis* = 10 : 90 at PSS. (b) UV/Vis absorption spectral changes of **9** (2.0 × 10^{-5} M in DMSO, 25 °C) upon irradiation at 365 nm.

3. Binding studies

Job's plots: $CDCl_3$ solvent was filtered through basic alumina prior to use. Stock solutions of equal concentration of azo compound (0.5 mM) and tetra-*n*-butylammonium chloride (TBACl, 0.5 mM) in 10% (v/v) DMSO-d_6/$CDCl_3$ saturated with water (< 0.1%) were prepared separately at 24 ± 1 °C. Keeping the total volume of 500 μL, aliquots of two stock solutions were added to an NMR tube in the following ratio; azo compound : anion = 10:0, 9:1, 8:2, 7:3, 6:4, 5:5, 4:6, 3:7, 2:8, and 1:9. Job's plots were constructed by plotting chemical shifts against mol fractions of the azo compound.

^{1}H NMR titrations: $CDCl_3$ solvent filtered through basic alumina prior to use. Stock solutions of azo compound (host, 5.0×10^{-4} M) and tetra-*n*-butylammonium chloride salt (guest, TBACl) (1.20×10^{-2} M) in 10% (v/v) DMSO-d_6/$CDCl_3$ saturated with water (< 0.1%) were prepared separately at 24 ± 1 °C. The stock solutions of trans isomers were covered with an aluminum foil in order to prevent the light exposure. For the titration of *cis* isomers, the host solution in a UV cell irradiated 365 nm of UV lamp (BLAK-RAY 100W mercury spot lamp) for more than 5 min. A 500 μL portion of the host solution was transferred to a NMR Tube, and an initial spectrum was taken to determine the chemical shift of free host. Aliquots of the guest solution (initially 10 μL, then 20-50 μL, and finally 250 μL) were added to the NMR tube and the spectrum was recorded after each addition. The association constants (K_a, M^{-1}) were determined by nonlinear least squares fitting of the titration curves[S6, 7], plotting the chemical shift changes of the (thio)urea NH signals against the concentrations (or equivalents) of the added chloride ion. Titration experiments were at least duplicated, and errors in the association constants were found to be less than 15% in all cases.

Calculation of binding constants: Azo compounds **1**-**9** exist in the thermally stable *trans* isomers predominantly (>98%), showing no appreciable ^{1}H NMR signals for the corresponding *cis* isomers unless exposing UV light. Therefore, the association constants between *trans* isomers and tetrabutylammonium chloride were determined by nonlinear least squares fitting analyses, assuming no *cis* isomers contained.

[S6] R. S. Macomber, *J. Chem. EducI.*, 1992, **69**, 375–378.
[S7] P. Thordarson, *Chem. Soc. Rev.*, 2011, **40**, 1305–1323.

On the other hand, the relative populations of *cis* isomers were in the range of 90-96% at photo-stationary states (PSS's) based on the ^{1}H NMR integrations, and the association constants between *cis* isomers and chloride were calculated by the combination of the following equations:

$$[H_0] = [H_{trans}] + [H_{cis}] + [H_{trans}G] + [H_{cis}G] \quad (1)$$

$$[G_0] = [H_{trans}G] + [H_{cis}G] + [G] \quad (2)$$

$$f = ([H_{cis}] + [H_{cis}G]) / [H_0] \quad (3)$$

$$K_{a,trans} = [H_{trans}G] / [H_{trans}][G] \quad (4)$$

$$K_{a,cis} = [H_{cis}G] / [H_{cis}][G] \quad (5)$$

Here, $[H_{cis}]$, $[H_{cis}G]$, $[H_{trans}]$, and $[H_{trans}G]$ are the concentrations of the free and complex of *cis* and *trans* isomer, respectively. f is the mole fraction of each *cis* isomer at the PSS, and $K_{a,trans}$ and $K_{a,cis}$ are the association constants of the *trans* and *cis* isomers, respectively.

The numerical solutions for the system of the five equations (1-5) were obtained by Newton's method and the algorithm was written in Visual Basic of Application.

First, a row matrix $\mathbf{X_i}$ having each variables of the system as elements was defined:

$$\mathbf{X_i} = ([H_{trans}] \quad [H_{cis}] \quad [G] \quad [H_{trans}G] \quad [H_{cis}G]) \quad (6)$$

Here, i is the number of repeating step and the initial values of $[H_{trans}]$, $[H_{cis}]$, $[G]$, $[H_{trans}G]$ and $[H_{cis}G]$ were all given as 0.0005.

Second, a column matrix $\mathbf{F_i}$ having function values of the system as elements was defined:

$$\mathbf{F_i} = \begin{pmatrix} F_1 \\ F_2 \\ F_3 \\ F_4 \\ F_5 \end{pmatrix} \quad (7)$$

Here, each function can be written as below:

$$F_1 = [H_{trans}] + [H_{cis}] + [H_{trans}G] + [H_{cis}G] - [H_0] \quad (8)$$

$$F_2 = [H_{trans}G] + [H_{cis}G] + [G] - [G_0] \quad (9)$$

$$F_3 = ([H_{cis}] + [H_{cis}G]) / [H_0] - f \quad (10)$$

$$F_4 = [H_{trans}G] / [H_{trans}][G] - K_{a,trans} \quad (11)$$

$$F_5 = [H_{cis}G] / [H_{cis}][G] - K_{a,cis} \quad (12)$$

Third, the Jacobian matrix $\mathbf{J_i}$ was defined:

$$\mathbf{J}_i = \begin{pmatrix} \frac{\partial F_1}{\partial [H_{trans}]} & \frac{\partial F_1}{\partial [H_{cis}]} & \frac{\partial F_1}{\partial [G]} & \frac{\partial F_1}{\partial [H_{trans}G]} & \frac{\partial F_1}{\partial [H_{cis}G]} \\ \frac{\partial F_2}{\partial [H_{trans}]} & \frac{\partial F_2}{[H_{cis}]} & \frac{\partial F_2}{\partial [G]} & \frac{\partial F_2}{\partial [H_{trans}G]} & \frac{\partial F_2}{\partial [H_{cis}G]} \\ \frac{\partial F_3}{\partial [H_{trans}]} & \frac{\partial F_3}{[H_{cis}]} & \frac{\partial F_3}{\partial [G]} & \frac{\partial F_3}{\partial [H_{trans}G]} & \frac{\partial F_3}{\partial [H_{cis}G]} \\ \frac{\partial F_4}{\partial [H_{trans}]} & \frac{\partial F_4}{[H_{cis}]} & \frac{\partial F_4}{\partial [G]} & \frac{\partial F_4}{\partial [H_{trans}G]} & \frac{\partial F_4}{\partial [H_{cis}G]} \\ \frac{\partial F_5}{\partial [H_{trans}]} & \frac{\partial F_5}{[H_{cis}]} & \frac{\partial F_5}{\partial [G]} & \frac{\partial F_5}{\partial [H_{trans}G]} & \frac{\partial F_5}{\partial [H_{cis}G]} \end{pmatrix} \quad (13)$$

$$\mathbf{J}_i \Delta \mathbf{X}_i = - \mathbf{F}_i \quad (14)$$

$$\Delta \mathbf{X}_i = - \mathbf{J}_i^{-1} \mathbf{F}_i \quad (15)$$

$$\mathbf{X}_{i+1} = \mathbf{X}_i + \Delta \mathbf{X}_i \quad (16)$$

The iteration process was repeated until $|\Delta X_i|$ is negligible, that is $|\Delta X_i| < 10^{-19}$.

The association constants of the *cis* isomers were determined by nonlinear least squares fitting analyses[S8] minimizing chi-squared values (χ^2):

$$\chi^2 = \Sigma(\Delta\delta_{calcd} - \Delta\delta_{obs})^2 \quad (17)$$

$$\Delta\delta_{obs} = \delta_{obs} - \delta_{free} \quad (18)$$

$$\Delta\delta_{calcd} = (\delta_{complex} - \delta_{free}) \times ([H_{cis}G] / [H_0]) \quad (19)$$

Here, δ_{obs} is the ^{1}H NMR chemical shift observed at each titration point, and δ_{free} and $\delta_{complex}$ are ^{1}H NMR chemical shifts of free and complex, respectively.

[S8] K.-J. Chang, Y.-J. An, H. Uh and K.-S. Jeong, *J. Org. Chem.*, 2004, **69**, 6556–6563.

Table S1. Association constants (K_a's, M^{-1}) between compounds **1-9** and tetrabutylammonium chloride in 10% (v/v) DMSO-d_6/$CDCl_3$ saturated by water (< 0.1%) at 298 K.

Compound	$K_{a,trans}$ (M^{-1})	*cis* ratio (%)	$K_{a,cis}$ (M^{-1})
1	–	–	–
2	34 ± 4	95	310 ± 20
3	–	–	–
4	140 ± 20	95	1040 ± 60
5	260 ± 40	95	1300 ± 100
6	410 ± 10	96	2800 ± 400
7	610 ± 20	90	5900 ± 800
8	570 ± 50	95	8400 ± 1000
9	820 ± 70	90	> 2×10^4

All titrations were at least duplicated, and one set of titration data for each compound is shown in Figure S10-S23.

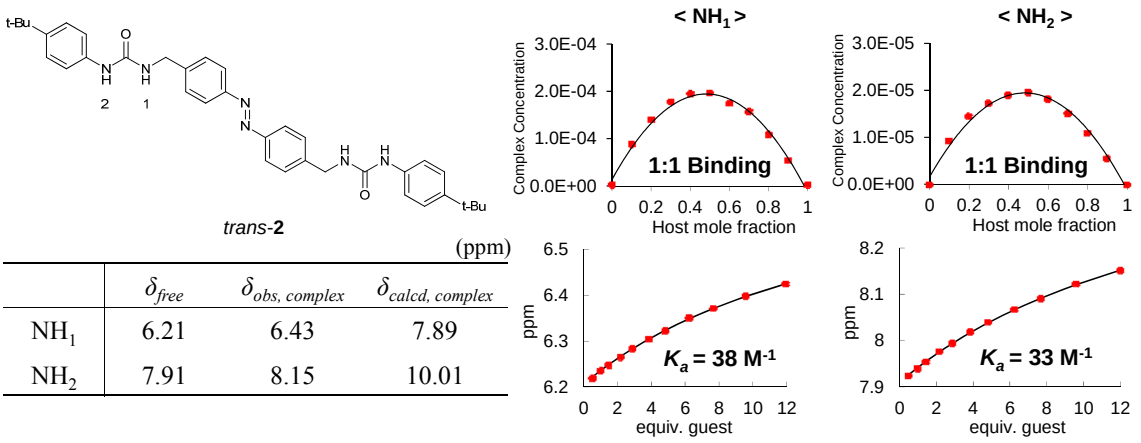

	δ_{free}	$\delta_{obs,\ complex}$	$\delta_{calcd,\ complex}$
NH_1	6.21	6.43	7.89
NH_2	7.91	8.15	10.01

Figure S10. Job's plots (right-top), titration curves (right-bottom, dot: experimental, line: theoretical values) and chemical shifts (left-bottom) of NH peaks of *trans*-**2**.

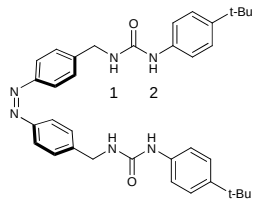

cis-**2**

(ppm)

	δ_{free}	$\delta_{obs,\ complex}$	$\delta_{calcd,\ complex}$
NH_1	6.15	6.48	6.80
NH_2	7.89	8.40	8.88

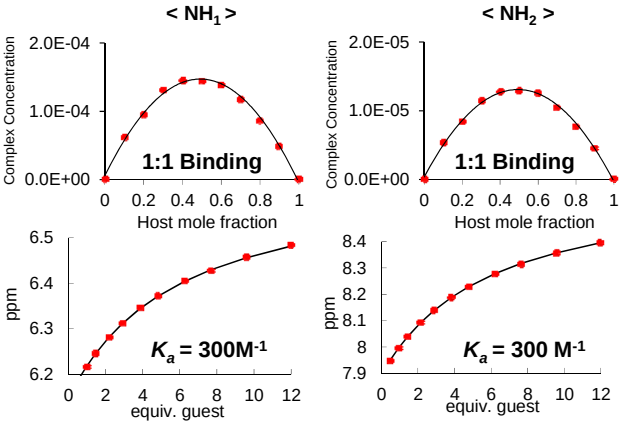

Figure S11. Job's plots (right-top), titration curves (right-bottom, dot: experimental, line: theoretical values) and chemical shifts (left-bottom) of NH peaks of *cis*-**2**.

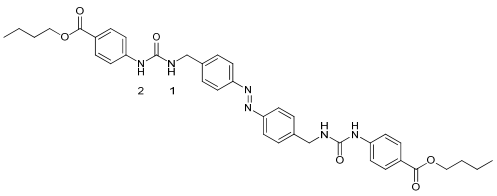

trans-**4**

(ppm)

	δ_{free}	$\delta_{obs,\ complex}$	$\delta_{calcd,\ complex}$
NH_1	6.41	6.86	7.57
NH_2	8.43	8.99	9.92

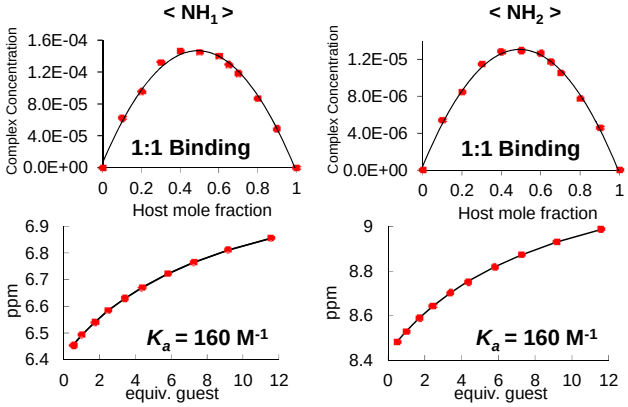

Figure S12. Job's plots (right-top), titration curves (right-bottom, dot: experimental, line: theoretical values) and chemical shifts (left-bottom) of NH peaks of *trans*-**4**.

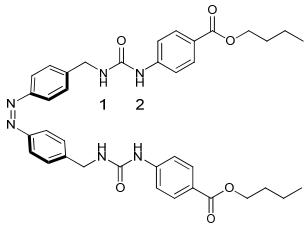

cis-**4**

(ppm)

	δ_{free}	$\delta_{obs,\ complex}$	$\delta_{calcd,\ complex}$
NH_1	6.35	6.81	6.96
NH_2	8.42	9.25	9.52

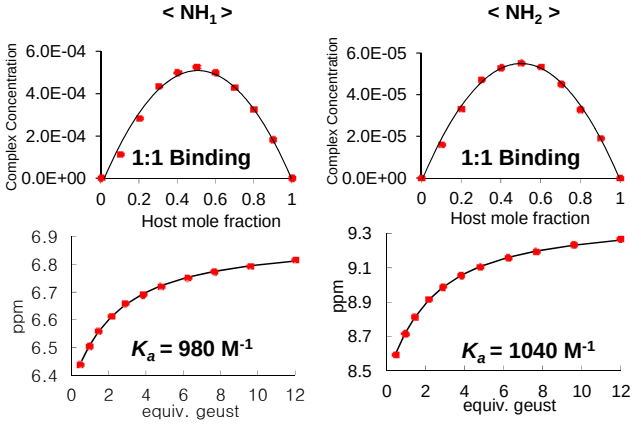

Figure S13. Job's plots (right-top), titration curves (right-bottom, dot: experimental, line: theoretical values) and chemical shifts (left-bottom) of NH peaks of *cis*-**4**.

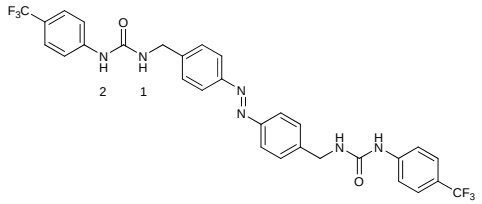

trans-**5**

(ppm)

	δ_{free}	$\delta_{obs,\ complex}$	$\delta_{calcd,\ complex}$
NH_1	6.39	6.71	7.13
NH_2	8.42	8.84	9.46

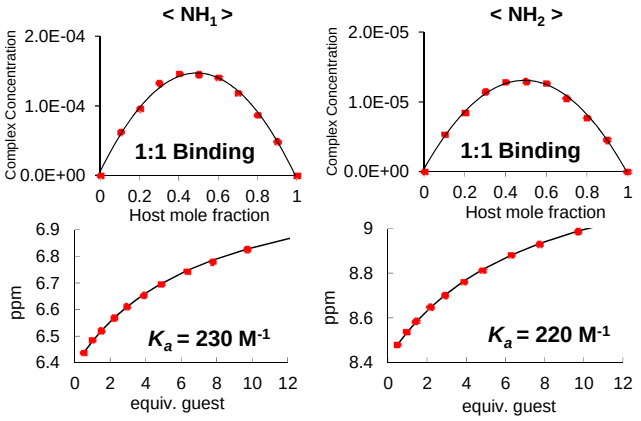

Figure S14. Job's plots (right-top), titration curves (right-bottom, dot: experimental, line: theoretical values) and chemical shifts (left-bottom) of NH peaks of *trans*-**5**.

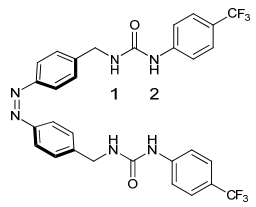

cis-**5**

(ppm)

	δ_{free}	$\delta_{obs,\ complex}$	$\delta_{calcd,\ complex}$
NH_1	6.34	6.75	6.90
NH_2	8.43	9.26	9.54

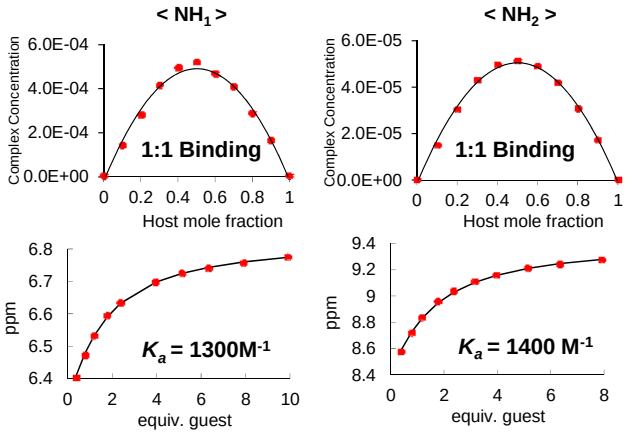

Figure S15. Job's plots (right-top), titration curves (right-bottom, dot: experimental, line: theoretical values) and chemical shifts (left-bottom) of NH peaks of *cis*-**5**.

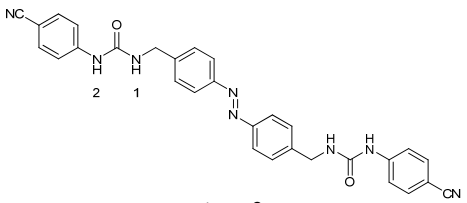

trans-**6**

(ppm)

	δ_{free}	$\delta_{obs,\ complex}$	$\delta_{calcd,\ complex}$
NH_1	6.44	7.01	7.40
NH_2	8.58	9.37	9.92

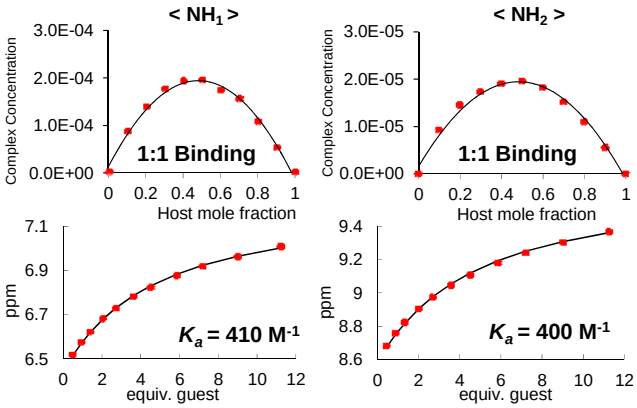

Figure S16. Job's plots (right-top), titration curves (right-bottom, dot: experimental, line: theoretical values) and chemical shifts (left-bottom) of NH peaks of *trans*-**6**.

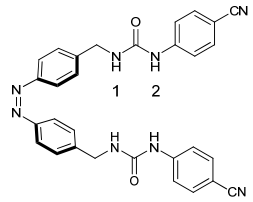

cis-**6**

(ppm)

	δ_{free}	$\delta_{obs,\ complex}$	$\delta_{calcd,\ complex}$
NH_1	6.38	6.81	6.86
NH_2	8.59	9.57	9.67

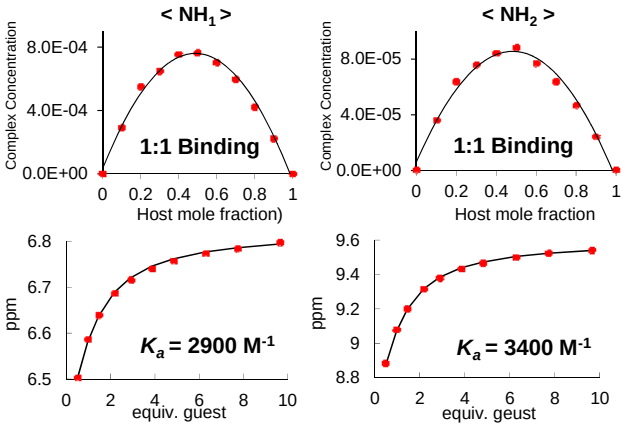

Figure S17. Job's plots (right-top), titration curves (right-bottom, dot: experimental, line: theoretical values) and chemical shifts (left-bottom) of NH peaks of *cis*-**6**.

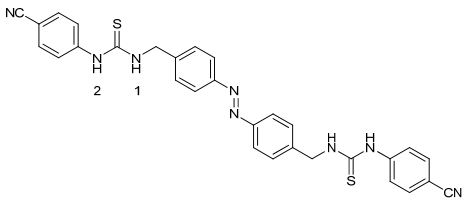

trans-**7**

(ppm)

	δ_{free}	$\delta_{obs,\ complex}$	$\delta_{calcd,\ complex}$
NH_1	7.96	8.81	9.17
NH_2	9.55	10.63	11.09

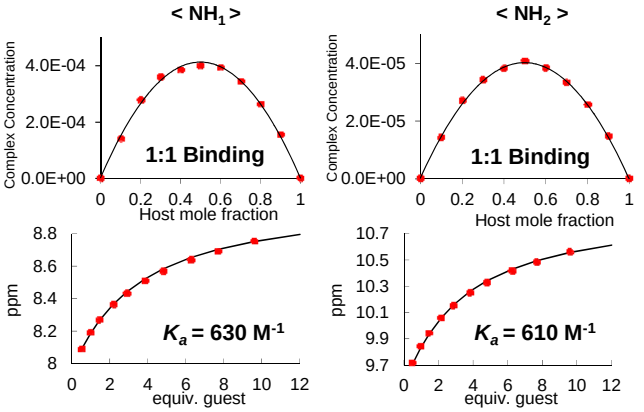

Figure S18. Job's plots (right-top), titration curves (right-bottom, dot: experimental, line: theoretical values) and chemical shifts (left-bottom) of NH peaks of *trans*-**7**.

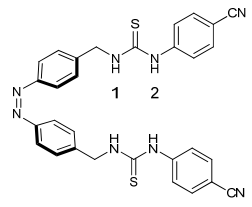

cis-**7**

(ppm)

	δ_{free}	$\delta_{obs,\ complex}$	$\delta_{calcd,\ complex}$
NH_1	7.90	8.37	8.43
NH_2	9.57	10.63	10.76

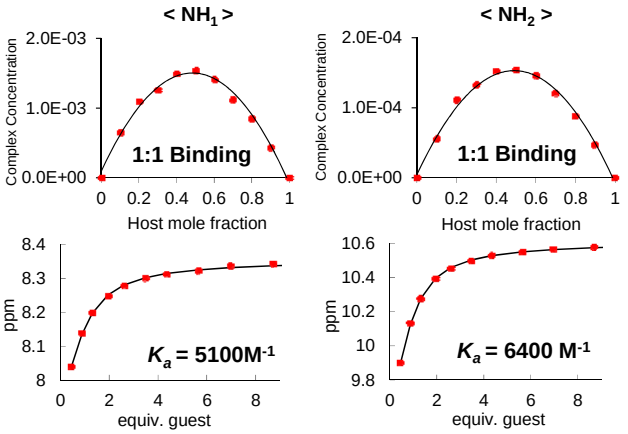

Figure S19. Job's plots (right-top), titration curves (right-bottom, dot: experimental, line: theoretical values) and chemical shifts (left-bottom) of NH peaks of *cis*-**7**.

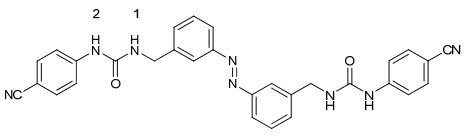

trans-**8**

(ppm)

	δ_{free}	$\delta_{obs,\ complex}$	$\delta_{calcd,\ complex}$
NH_1	6.48	7.02	7.26
NH_2	8.58	9.36	9.73

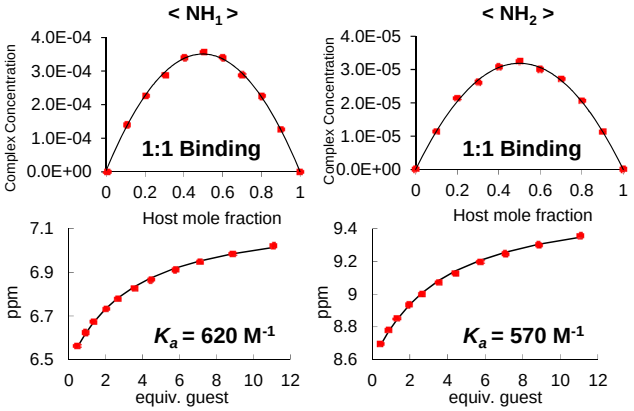

Figure S20. Job's plots (right-top), titration curves (right-bottom, dot: experimental, line: theoretical values) and chemical shifts (left-bottom) of NH peaks of *trans*-**8**.

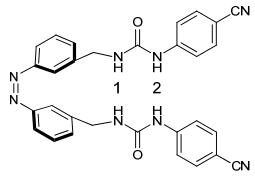

cis-**8**

(ppm)

	δ_{free}	$\delta_{obs,\ complex}$	$\delta_{calcd,\ complex}$
NH_1	6.32	7.02	7.08
NH_2	8.53	9.46	9.53

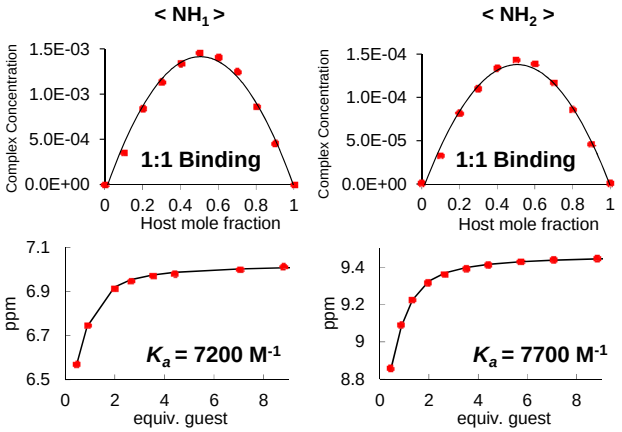

Figure S21. Job's plots (right-top), titration curves (right-bottom, dot: experimental, line: theoretical values) and chemical shifts (left-bottom) of NH peaks of *cis*-**8**.

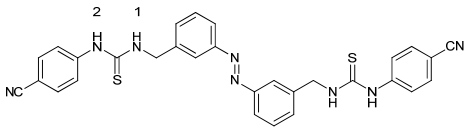

trans-**9**

(ppm)

	δ_{free}	$\delta_{obs,\ complex}$	$\delta_{calcd,\ complex}$
NH_1	8.01	8.78	8.98
NH_2	9.56	10.56	10.82

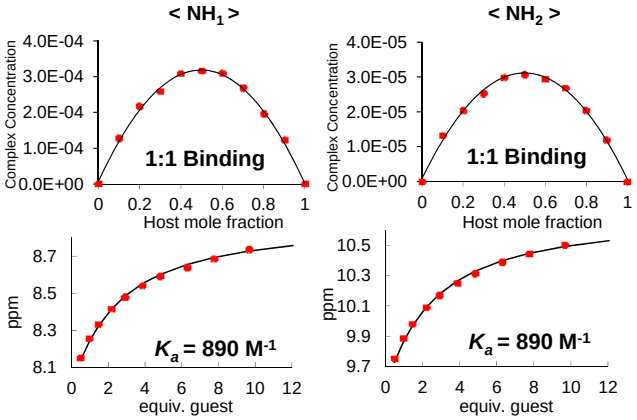

Figure S22. Job's plots (right-top), titration curves (right-bottom, dot: experimental, line: theoretical values) and chemical shifts (left-bottom) of NH peaks of *trans*-**9**.

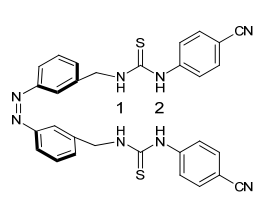

cis-**9**

(ppm)

	δ_{free}	$\delta_{obs,\ complex}$	$\delta_{calcd,\ complex}$
NH_1	7.89	8.62	8.70
NH_2	9.54	10.39	10.47

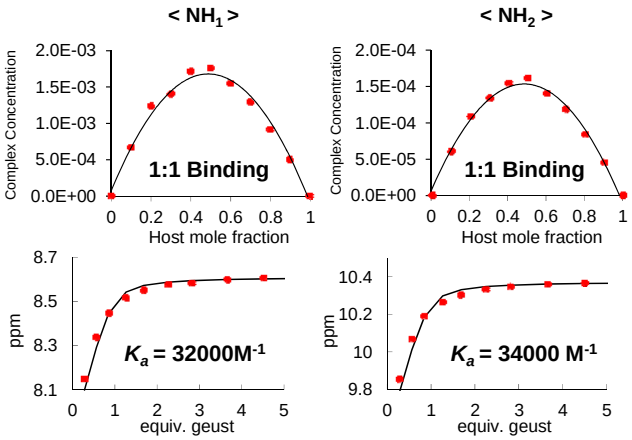

Figure S23. Job's plots (right-top), titration curves (right-bottom, dot: experimental, line: theoretical values) and chemical shifts (left-bottom) of NH peaks of *cis*-**9**.

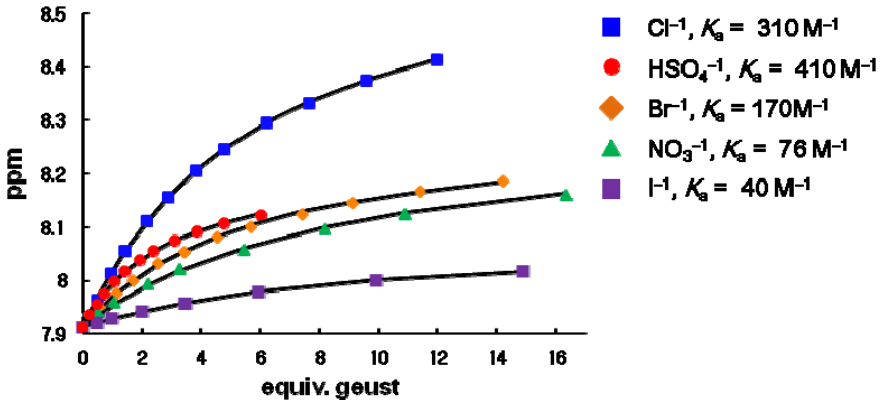

Figure S24. Titration curves of experimental (dots) and theoretical (lines) ones with *cis*-**2** and tetrabutylammonium anions in 10% (v/v) DMSO-d_6/$CDCl_3$ saturated with water (< 0.1%)

4. Transport experiments

Preparation of lipid vesicles. A chloroform solution (15 mL) of 1-palmitoyl-2-oleoylphosphatidylcholine (POPC) (30 mg) was evaporated under reduced pressure to give a thin film. The lipid film was dried under high vacuum overnight. The thin film was rehydrated by vortexing with a sodium chloride solution (500 mM NaCl, 5 mM phosphate buffer at pH = 7.2, 1 mL). The lipid suspension was then subjected to nine freeze–thaw cycles and was allowed to age for 1 h at room temperature. The suspension was extruded twenty-three times through a 200 nm polycarbonate membrane using extruder (Avanti, The Mini-Extruder set) to obtain unilamellar vesicles containing NaCl (500 mM in 5 mM phosphate buffer at pH = 7.2). Non-encapsulated NaCl salts were removed by dialysing the vesicles three times in a sodium nitrate solution (500 mM $NaNO_3$, 5 mM phosphate buffer at pH = 7.2, 100 mL).

Transport experiments using POPC vesicles. First, stock solutions (4 mM) of azo compounds in dimethyl sulfoxide (DMSO, 350-550 μL) were prepared prior to transport experiments. The stock solutions were covered with aluminium foil to maximize thermally stable *trans* isomers (> 98%). On the other hand, the solutions were irradiated for 5 min with an ultraviolet lamp (365 nm, BLAK-RAY 100 W mercury spot lamp, Ted Pella, Inc.) to afford the *cis* isomers with the maximal populations (90-96%).

Next, the vesicles solution prepared above were suspended in an external solution (500 mM $NaNO_3$ or 166 mM Na_2SO_4 containing 5 mM $NaHCO_3$ in 5 mM phosphate buffer at pH = 7.2, 40 mL). The total lipid concentration was 1 mM. An aliquot (10 μL) of the DMSO solution of a carrier (4 mM) was added, and the chloride efflux from vesicles was monitored for 400 or 600 sec using a chloride selective electrode (Thermo Scientific Orion DUAL STAR^{TM} pH/ISE Meter, 9617BNWP). The initial reading at t = 0 was considered as 0% release of chloride ions and the reading after the addition of 10% Triton X-100 to the lipid solution at t = 400 or 600 sec was considered as 100% release. When the solution was irradiated by UV light *in situ* on the transport experiment, the electrode should be pulled out from the solution when irradiated. The chloride efflux was recorded until t = 120 sec, and then the solution was irradiated for 20 sec with an ultraviolet lamp (365 nm, BLAK-

RAY 100 W mercury spot lamp, Ted Pella, Inc.).

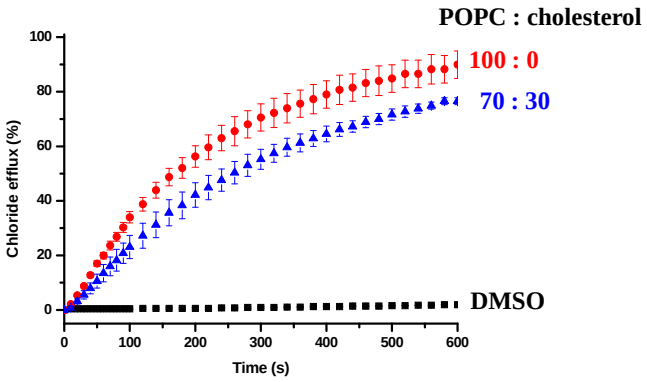

Figure S25. Comparison of chloride efflux facilitated by *cis*-**6** (2 mol% of carrier to lipid) between 100% POPC and 70:30 POPC/cholesterol vesicles (500 mM NaCl in 5 mM phosphate buffer at pH = 7.2).

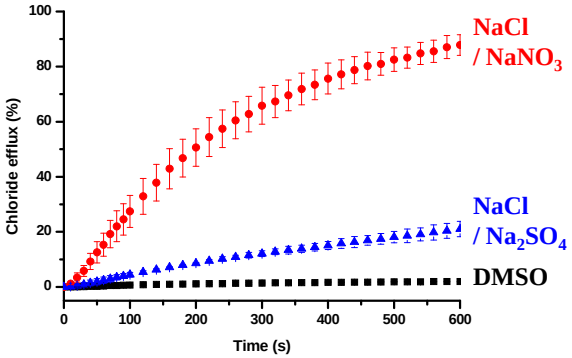

Figure S26. Chloride efflux facilitated by *cis*-**6** (2 mol% of carrier to lipid) from POPC vesicles to different extravesicular solutions containing $NaNO_3$ (500 mM) or Na_2SO_4 (166 mM) buffered to pH 7.2 with 5 mM phosphate salts.

5. Hill analyses of chloride transport

Hill analyses were performed to quantify the chloride transport abilities of compounds **1**-**9**.[S9] For various concentrations of the compound, the chloride efflux (%) was measured. Data points were fitted to the Hill equation using Origin 8.0:

$$y = V_{max}\{ x^n / (k^n + x^n)\} = 100\%\{ x^n / (EC_{50}{}^n + x^n)\}$$

Where y is the chloride efflux at 300 s (%) and x is the compounds concentration (mol% to lipid). V_{max} is the maximum efflux possible, n is the Hill coefficient and k is the concentration needed to reach half of V_{max} (k equals EC_{50}). This enables us to calculate $EC_{50,\ 300s}$ values, defined as the concentration of compounds required to achieve 50% chloride efflux at 300 s after addition of compounds.

Table S2. Results of Hill analyses of *cis*-**1**-**9**.

Compound	EC_{50} (mol%)	Error of EC_{50} (mol%)	n	Error of n
cis-**1**	5.339	0.176	1.59	0.09
cis-**2**	–[a]	–[a]	–[a]	–[a]
cis-**3**	4.620	0.149	1.24	0.05
cis-**4**	–[a]	–[a]	–[a]	–[a]
cis-**5**	2.350	0.227	1.08	0.12
cis-**6**	1.128	0.063	1.07	0.06
cis-**7**	0.191	0.011	1.48	0.17
cis-**8**	0.381	0.011	0.90	0.03
cis-**9**	0.148	0.013	1.22	0.16

[a] not determined due to low activities.

[S9] N. Busschaert, I. L. Kirby, S. Young, S. J. Coles, P. N. Horton, M. E. Light and P. A. Gale, *Angew. Chem. Int. Ed*., 2012, **51**, 4426–4430.

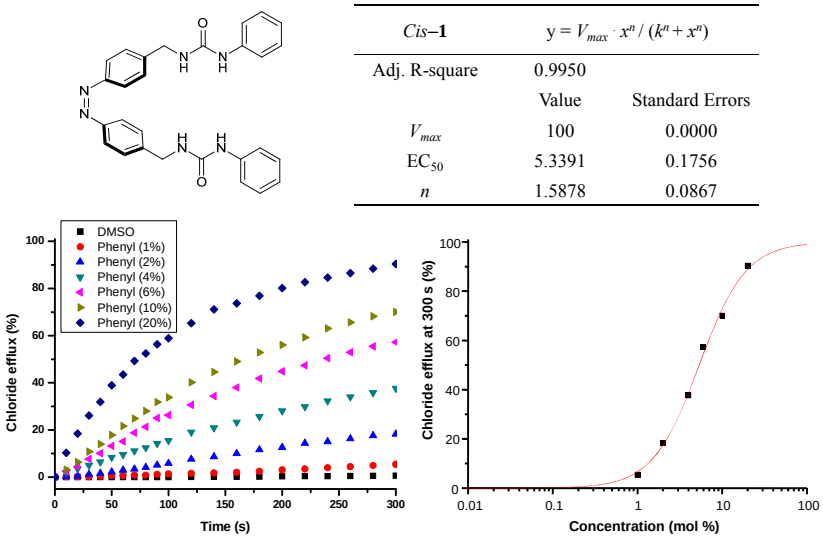

Cis–**1**	$y = V_{max} \cdot x^n / (k^n + x^n)$	
Adj. R-square	0.9950	
	Value	Standard Errors
V_{max}	100	0.0000
EC_{50}	5.3391	0.1756
n	1.5878	0.0867

Figure S27. Hill plots were performed for various concentrations of *cis*-**1** (1.0, 2.0, 4.0, 6.0, 10.0 and 20.0 mol% of carrier to lipid in DMSO) respectively (left-bottom). Data points were fitted to the Hill equation using Origin 8.0 (right-bottom).

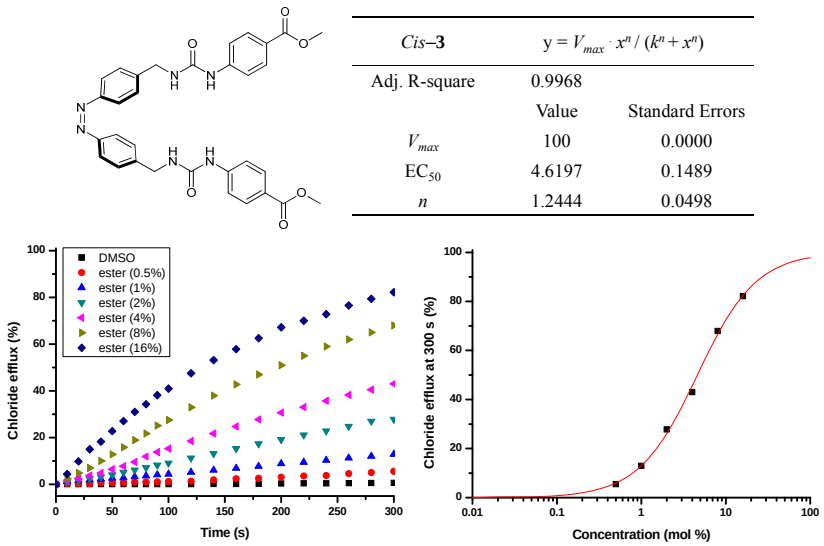

Cis–**3**	$y = V_{max} \cdot x^n / (k^n + x^n)$	
Adj. R-square	0.9968	
	Value	Standard Errors
V_{max}	100	0.0000
EC_{50}	4.6197	0.1489
n	1.2444	0.0498

Figure S28. Hill plots were performed for various concentrations of *cis*-**3** (0.5, 1.0, 2.0, 4.0, 8.0 and 16.0 mol% of carrier to lipid in DMSO) respectively (left-bottom). Data points were fitted to the Hill equation using Origin 8.0 (right-bottom).

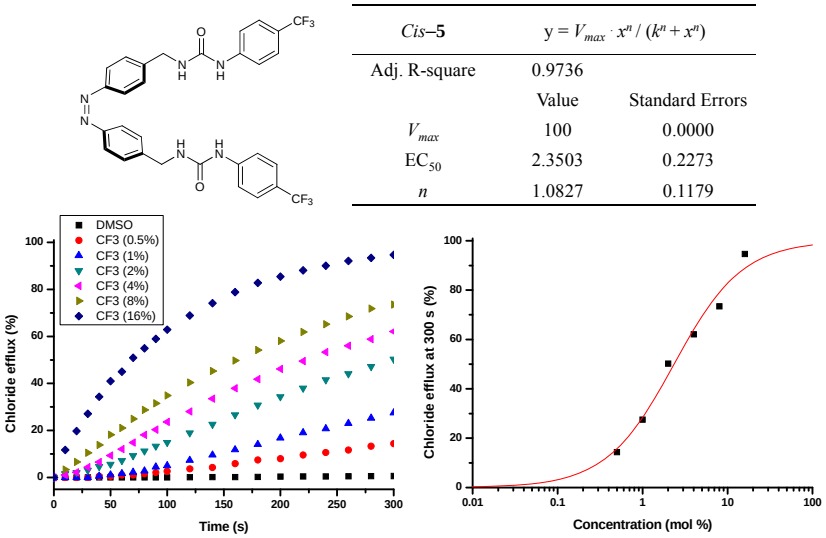

Cis–**5**	$y = V_{max} \cdot x^n / (k^n + x^n)$	
Adj. R-square	0.9736	
	Value	Standard Errors
V_{max}	100	0.0000
EC_{50}	2.3503	0.2273
n	1.0827	0.1179

Figure S29. Hill plots were performed for various concentrations of *cis*-**5** (0.5, 1.0, 2.0, 4.0, 8.0 and 16.0 mol% of carrier to lipid in DMSO) respectively (left-bottom). Data points were fitted to the Hill equation using Origin 8.0 (right-bottom).

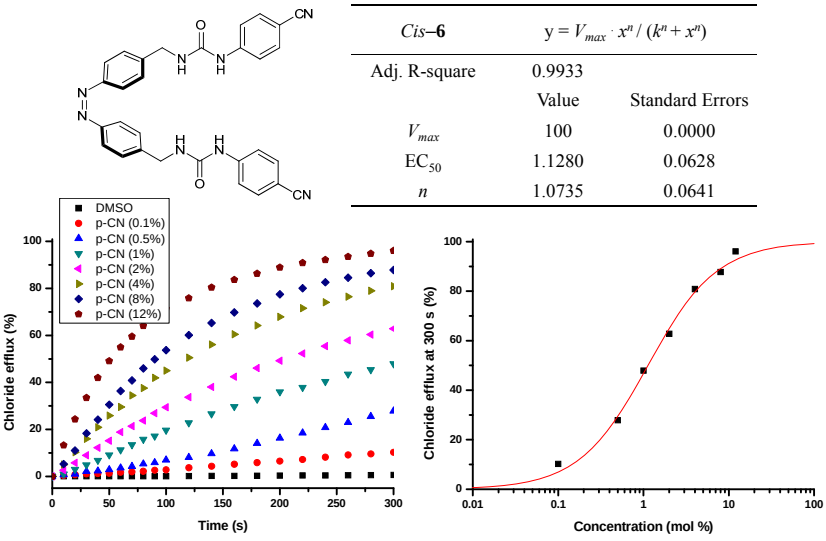

Cis–**6**	$y = V_{max} \cdot x^n / (k^n + x^n)$	
Adj. R-square	0.9933	
	Value	Standard Errors
V_{max}	100	0.0000
EC_{50}	1.1280	0.0628
n	1.0735	0.0641

Figure S30. Hill plots were performed for various concentrations of *cis*-**6** (0.1, 0.5, 1.0, 2.0, 4.0, 8.0 and 12.0 mol% of carrier to lipid in DMSO) respectively (left-bottom). Data points were fitted to the Hill equation using Origin 8.0 (right-bottom).

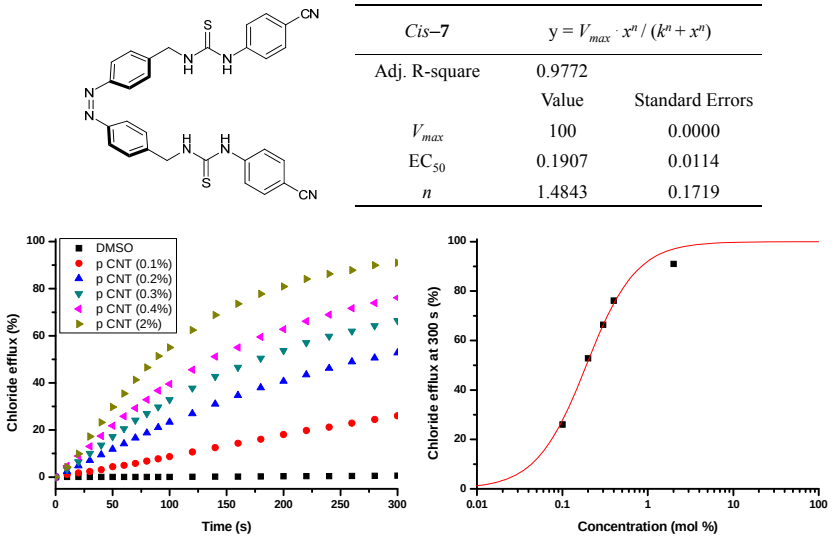

Cis–**7**	$y = V_{max} \cdot x^n / (k^n + x^n)$	
Adj. R-square	0.9772	
	Value	Standard Errors
V_{max}	100	0.0000
EC_{50}	0.1907	0.0114
n	1.4843	0.1719

Figure S31. Hill plots were performed for various concentrations of *cis*-**7** (0.1, 0.2, 0.3, 0.4 and 2.0 mol% of carrier to lipid in DMSO) respectively (left-bottom). Data points were fitted to the Hill equation using Origin 8.0 (right-bottom).

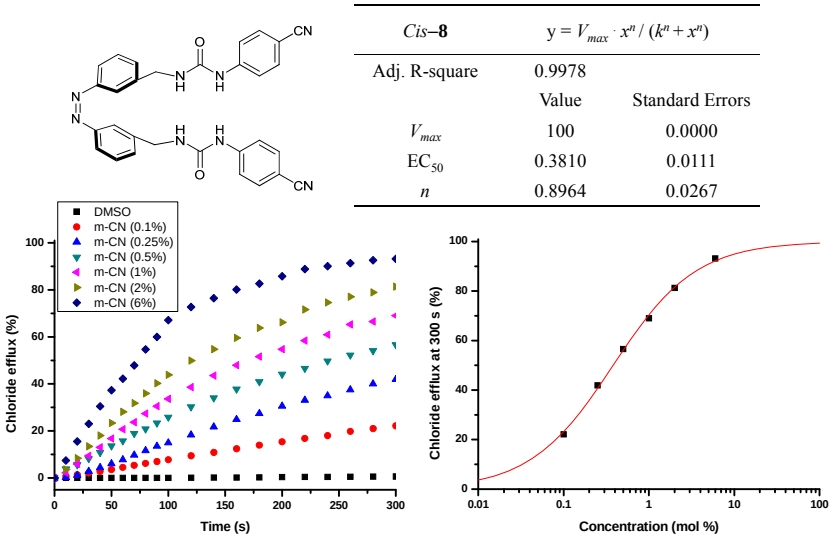

Cis–**8**	$y = V_{max} \cdot x^n / (k^n + x^n)$	
Adj. R-square	0.9978	
	Value	Standard Errors
V_{max}	100	0.0000
EC_{50}	0.3810	0.0111
n	0.8964	0.0267

Figure S32. Hill plots were performed for various concentrations of *cis*-**8** (0.1, 0.25, 0.5, 1.0, 2.0 and 6.0 mol% of carrier to lipid in DMSO) respectively (left-bottom). Data points were fitted to the Hill equation using Origin 8.0 (right-bottom).

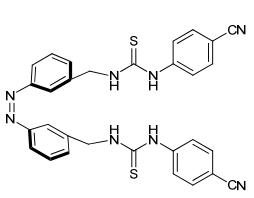

Cis–**9**	$y = V_{max} \cdot x^n / (k^n + x^n)$	
Adj. R-square	0.9662	
	Value	Standard Errors
V_{max}	100	0.0000
EC_{50}	0.1479	0.0125
n	1.2236	0.1639

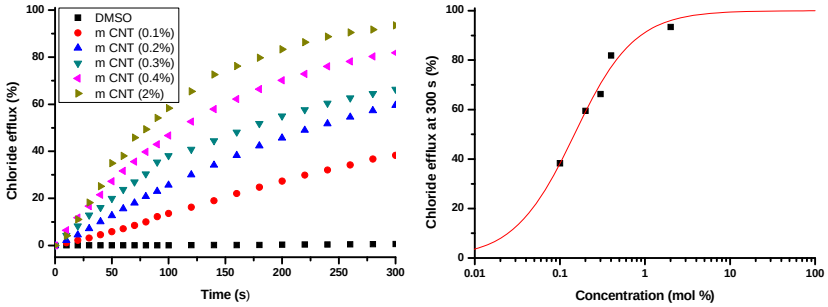

Figure S33. Hill plots were performed for various concentrations of *cis*-**9** (0.1, 0.2, 0.3, 0.4 and 2.0 mol% of carrier to lipid in DMSO) respectively (left-bottom). Data points were fitted to the Hill equation using Origin 8.0 (right-bottom).

6. *In vitro* chloride transport experiments

a) Chloride transport across plasma membrane

Cell culture: FRT cells were stably transfected with the halide sensor YFP. The cells were plated in 96-well black-walled microplates (Corning, Corning, NY, USA) at a density of 20,000 cells/well in Coon's modified F12 medium supplemented with 10% FBS, 100 U/mL penicillin and 100 μg/mL streptomycin and then incubated for 48 hours at 37 ^{o}C in 5% CO_2/95% air.

Measurement of $[Cl^-]_i$: Changes in intracellular chloride ion concentration were measured by the halide sensor YFP-F46L/H148Q/I152L. 96-well microplates containing FRT cells expressing YFP-F46L/H148Q/I152L were washed 3 times with PBS (200 μL/wash). After washing with PBS, 100 μL of the HEPES-buffered solution (pH= 7.4) containing 140 mM NaCl, 5 mM KCl, 1mM $MgCl_2$, 10 mM HEPES, 1 mM $CaCl_2$, 10 mM D-glucose was added to each well of the 96-well microplates. Each cell was exposed to *trans* or *cis* isomers of **6**-**9** (30 μM) and changes in the intracellular chloride concentration were measured by YFP fluorescence every 10 min with the excitation wavelength of 485 nm and the emission wavelength of 530 nm at 298 K. The YFP fluorescence images were captured by IncuCyte™ ZOOM (Essen BioScience, Inc. U.S.A.), a live content imaging system, and analyzed using image analysis software (Meta Imaging Series 7.7).

Initial fluorescence intensity of each image was obtained from the instruments automatically, and the intensity was corrected by subtracting the background fluorescence originated from the well without cells. To compare the relative fluorescence decrease, the intensity at time was divided by the intensity at time = 0 ($I = I_t/I_0$ x 100). The experiments were repeated six times (n = 30), and the average values are shown as a bar graph (Fig. 3b).

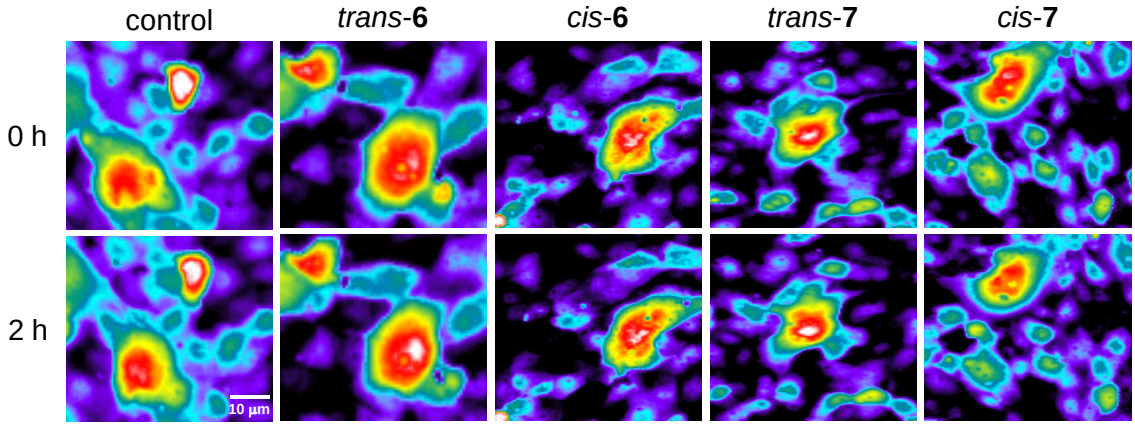

Figure S34. Fluorescence changes of YFP-transfected FRT cells after 2 h exposure to compounds **6** and **7** (30 µM).